PAPER Special Issue on Spread Spectrum Techniques and Applications

Performance of Asynchronous Band-Limited DS/SSMA Systems

Takafumi SHIBATA†, Masaaki KATAYAMA†† *and* Akira OGAWA††, *Members*

SUMMARY This paper discusses the performance of asynchronous direct-sequence spread-spectrum multiple-access systems using binary or quaternary phase-shift keyed signals with the strict bandwidth-limitation by Nyquist filtering. The signal-to-noise plus interference ratio (SNIR) at the output from the correlation receiver is derived analytically taking the cross-correlation characteristics of spreading sequences into account, and also an approximated SNIR of a simple form is presented for the systems employing Gold sequences. Based on the analyzed result of SNIR, bit error rate performance and spectral efficiency are also estimated.

key words: *direct-sequence spread-spectrum multiple-access, signal-to-noise plus interference ratio, band-limitation, spectral efficiency, gold sequence*

1. Introduction

Direct-sequence spread-spectrum multiple-access (DS/SSMA) systems draw much attention because of the attractive features such as easiness of overcoming interference and multipath effect, and capability of asynchronous access.

Since spread-spectrum signals should have wide bandwidth and low power spectral density, the effects of the system band-limitation have been often neglected. In DS/SSMA systems, however, numerous signals are transmitted at the same time and the total out-of-band emission power may become very large, even though each signal has a little out-of-band emission. Thus the signals have to be strictly band-limited to avoid interference to other systems in the adjacent frequency-bands.

Several studies have been made on the performance of band-limited DS/SSMA systems [1]-[3]. It does not appear to us, however, that there have been analytical results of asynchronous band-limited DS/SSMA systems taking the cross-correlation characteristics of actual spreading sequences into consideration. Almost all of previous works are made by simulation or the analysis in which the random spreading sequences are assumed.

The objective of this paper is to evaluate the performance of a practical band-limited DS/SSMA system analytically taking account of the cross-correlation characteristics of spreading sequences. For this purpose, the signal-to-noise plus interference ratio (SNIR) of the despread signal, as a measure of performance, is derived for the system, in which binary phase-shift keyed (BPSK) signals or quaternary phase-shift keyed (QPSK) signals are band-limited by Nyquist filtering. Then, Gold sequence, which is most commonly used for spectrum-spreading, is applied and an approximation of the performance of a very simple form is derived.

As examples of application, we also estimate the bit error rate performance and the spectral efficiency using the analyzed result of SNIR.

2. System Model

The models of band-limited DS/SSMA systems with BPSK and QPSK are shown in Figs. 1(a) and (b), respectively.

To begin with, let us consider the BPSK system. It is assumed that the number of users is K and these users have access asynchronously to the system with the same signal power. At the BPSK transmitter for k-th user ($1 \leqq k \leqq K$), the information signal $b_k(t)$, which has a rectangular waveform of duration T and takes the value $+1$ or -1, is first multiplied by the spreading signal,

$$a_k(t) = \sum_{l=-\infty}^{\infty} a_{k,l}\, c(t - lT_c), \tag{1}$$

where $\{a_{k,l}\}$ is the spreading sequence assigned for the k-th user's signal which takes the values $+1$ or -1, and

$$c(t) = \begin{cases} 1 & ; \quad |t| \leqq \dfrac{T_c}{2} \\ 0 & ; \quad \text{otherwise.} \end{cases} \tag{2}$$

The period of the spreading sequence $\{a_{k,l}\}$ is set to be $N = T/T_c$, which is the number of chips in one-bit duration of $b_k(t)$.

After the spreading, the signal $b_k(t)\, a_k(t)$ is BPSK-modulated and gives

$$g_k(t) = \sqrt{2P}\, b_k(t)\, a_k(t) \cos(\omega_c t + \beta_k), \tag{3}$$

Manuscript received January 11, 1993.
Manuscript revised April 5, 1993.

† The author is with NTT Mobile Communications Network Inc., Tokyo, 105 Japan.
†† The authors are with the Faculty of Engineering, Nagoya University, Nagoya-shi, 464-01 Japan.

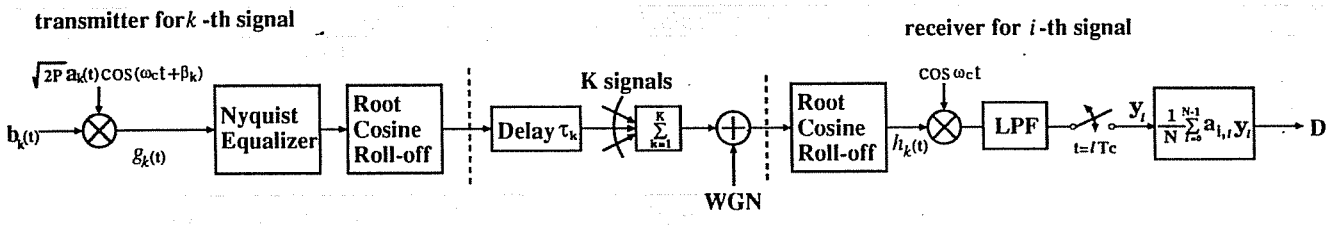

(a) BPSK System

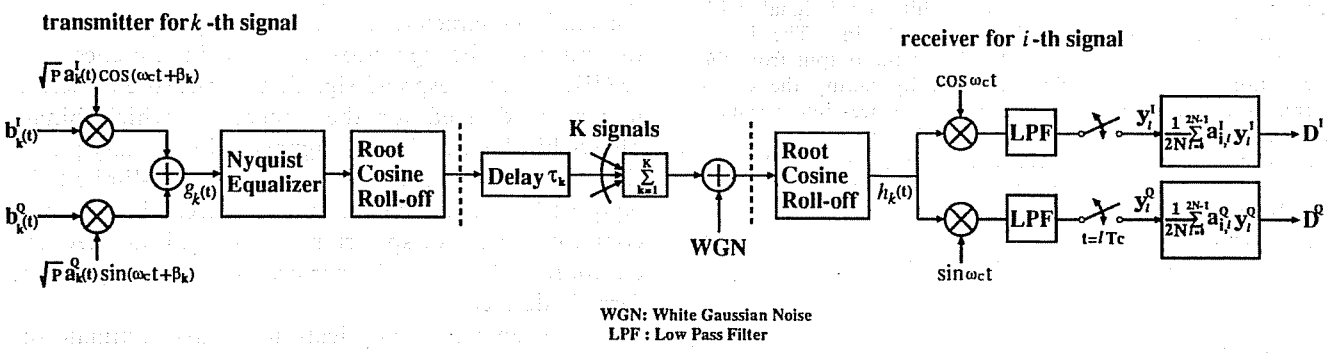

(b) QPSK System

Fig. 1 System models.

where P is the signal power, ω_c is the carrier frequency in common among K signals, and β_k is an initial phase of the k-th user's signal.

The bandwidth of this signal is very wide and has large side lobes, because $b_k(t)\,a_k(t)$ is the sequence of rectangular pulses; therefore, the signal $g_k(t)$ has to be band-limited. In this paper, we employ the Nyquist spectrum shaping with a raised cosine frequency response $X(\omega)$, which is evenly divided between the transmitter and the receiver. This type of spectrum shaping is essential, as it provides an effective band-limitation with no intersymbol interference. As $X(\omega)$ is evenly divided, transmit filter, preceded by the aperture equalizer, has the square-root raised-cosine shaped frequency response $\sqrt{X(\omega-\omega_c)}$.

The equivalent lowpass frequency responses of the raised-cosine shaping, $X(\omega)$, and that of the aperture equalizer, $E_q(\omega)$, are given below.

$$X(\omega)=\begin{cases}1 & ;\ |\omega|\leqq\dfrac{\pi}{T_c}(1-\alpha)\\ \dfrac{1}{2}\left[1-\sin\left\{\dfrac{T_c}{2\alpha}\left(\omega-\dfrac{\pi}{T_c}\right)\right\}\right] & ;\ \dfrac{\pi}{T_c}(1-\alpha)\leqq\omega\leqq\dfrac{\pi}{T_c}(1-\alpha)\\ \dfrac{1}{2}\left[1+\sin\left\{\dfrac{T_c}{2\alpha}\left(\omega+\dfrac{\pi}{T_c}\right)\right\}\right] & ;\ -\dfrac{\pi}{T_c}(1+\alpha)\leqq\omega\leqq-\dfrac{\pi}{T_c}(1-\alpha)\\ 0 & ;\ |\omega|\leqq\dfrac{\pi}{T_c}(1+\alpha)\end{cases} \tag{4}$$

$$E_q(\omega)=\begin{cases}\left[S_a\left(\dfrac{\omega T_c}{2}\right)\right]^{-1} & ;\ |\omega|\leqq\dfrac{\pi}{T_c}(1+\alpha)\\ 0 & ;\ \text{otherwise}\end{cases} \tag{5}$$

where α is the roll-off factor and $S_a(x)$ is the sampling function given by

$$S_a(x)=\frac{\sin x}{x}. \tag{6}$$

The received signals, corrupted by interferences from other spread-spectrum signals and thermal noise, are filtered by the receive filter with the same frequency

response as the transmit filter, coherently demodulated, and sampled at each chip timing. Then the sampled chip data y_l are correlated discretely to the desired code sequence $\{a_{i,l}\}$ as is shown in Fig. 1, in which the signal from the i-th user is assumed to be the desired one.

Next, let us show the system with QPSK modulation. For QPSK, Eq. (3) should be replaced by

$$g_k(t)=\sqrt{P}b_k^I(t)\,a_k^I(t)\cos(\omega_c t+\beta_k)+\sqrt{P}b_k^Q(t)\,a_k^Q(t)\sin(\omega_c t+\beta_k) \tag{7}$$

where $b_k^I(t)$, $a_k^I(t)$ and $b_k^Q(t)$, $a_k^Q(t)$ are the information signals and the spreading signals for the in-phase and quadrature components, respectively. The spreading sequences assigned for $a_k^I(t)$ and $a_k^Q(t)$ are represented by $\{a_{k,l}^I\}$ and $\{a_{k,l}^Q\}$.

For the purpose of comparison, it is assumed that the data rate, the power and the bandwidth of the QPSK signals are the same as those of the BPSK signal. Since the bandwidth of the BPSK and QPSK systems is assumed to be the same, the chip rate of the spreading sequences $a_k(t)$, $a_k^I(t)$, and $a_k^Q(t)$ are also the same. On the other hand, as the symbol rate of the QPSK signal is half the rate of the BPSK signal, the symbol duration of QPSK becomes $2T$. Accordingly, the period of $\{a_{k,l}^I\}$ and $\{a_{k,l}^Q\}$, which is the same as the number of the chips included in one-bit duration of the information signals $b_k^I(t)$ and $b_k^Q(t)$, becomes $2N$.

3. Performance Analysis

3.1 BPSK

At the receiver, K signals arrive with white Gaussian noise. In order to simplify the analysis, let us assume that $b_k(t)$ is fixed at $+1$ and each incoming signal has the same power. The signals which have the square-root raised-cosine shaped spectrum are first filtered by the receive filter with the frequency response $\sqrt{X(\omega-\omega_c)}$. Thus the k-th signal component at the output from the receive filter is of the following form:

$$h_k(t)=\sqrt{2P}\left\{\sum_{m=-\infty}^{+\infty}a_{k,m}\cdot x(t-mT_c-\tau_k)\right\}\cdot\cos(\omega_c t+\phi_k) \tag{8}$$

where $x(t)$ is the impulse response of $X(\omega)$, and is expressed as

$$x(t)=\frac{1}{1-4\alpha^2t^2/T_c^2}\left[\frac{1+\alpha}{2}\cdot\mathrm{Sa}\left\{\pi(1+\alpha)\frac{t}{T_c}\right\}+\frac{1-\alpha}{2}\cdot\mathrm{Sa}\left\{\pi(1-\alpha)\frac{t}{T_c}\right\}\right]. \tag{9}$$

The time delay τ_k and the carrier phase ϕ_k for k-th signal are independent random variables uniformly distributed over $[0,\ NT_c]$ and $[0,\ 2\pi]$, respectively. Since τ_k and ϕ_k for different k are independent, we can assume that each signal after the receive filter is also independent.

Considering the signal from the i-th user as desired one, we assume that any synchronization necessary for the reception of the i-th signal has been perfectly established, and both ϕ_i and τ_i are set to be zero. The desired signal component of the correlator output, D_i, is thus

$$D_i=\frac{1}{N}\sum_{l=0}^{N-1}a_{i,l}\cdot\sqrt{\frac{P}{2}}a_{i,l}=\sqrt{\frac{P}{2}}. \tag{10}$$

The correlator output for the k-th signal D_k, which is an interference against i-th channel signal, is expressed as

$$D_k=\sqrt{\frac{P}{2}}\cos\phi_k\left[\frac{1}{N}\sum_{l=0}^{N-1}\left\{a_{i,l}\cdot\sum_{m=-\infty}^{+\infty}a_{k,m}\cdot x(lT_c-mT_c-\tau_k)\right\}\right]. \tag{11}$$

Replacing $l-m$ by q and taking periodicity of $\{a_{k,m}\}$ into account, we obtain

$$D_k=\frac{1}{N}\sqrt{\frac{P}{2}}\cos\phi_k\sum_{q=-\infty}^{+\infty}\theta_{k,i}(q)\cdot x(qT_c-\tau_k), \tag{12}$$

where

$$\theta_{k,i}(q)=\sum_{l=0}^{N-1}a_{i,l}\cdot a_{k,N-q+l}=\theta_{k,i}(q+N). \tag{13}$$

From these equations, the variance of D_k can be obtained as

$$\mathrm{Var}[D_k]=\int_0^{NT_c}\int_0^{2\pi}D_k^2\frac{d\tau_k}{NT_c}\frac{d\phi_k}{2\pi}=\frac{P}{4N^3T_c}\sum_{q=-\infty}^{+\infty}\sum_{q'=-\infty}^{+\infty}\theta_{k,i}(q)\cdot\theta_{k,i}(q')\cdot\psi(q,\,q'), \tag{14}$$

where

$$\psi(q,\,q')=\int_{(q-N)T_c}^{qT_c}x(\tau)\cdot x(\tau+(q'-q)\,T_c)\,d\tau. \tag{15}$$

Replacing $q'-q$ by r and q by $Nu+s$, (u, s: integers) and taking the periodicity of $\theta_{k,i}(q)$ into account, we can modify (14) as

$$\mathrm{Var}[D_k]=\frac{P}{4N^3T_c}\sum_{u=-\infty}^{+\infty}\sum_{s=0}^{N-1}\sum_{r=-\infty}^{+\infty}\theta_{k,i}(Nu+s)\cdot\theta_{k,i}(Nu+s+r)\cdot\int_{\{N(u-1)+s\}T_c}^{\{Nu+s\}T_c}x(\tau)\cdot x(\tau+rT_c)\,d\tau=\frac{P}{4N^3T_c}\sum_{r=-\infty}^{+\infty}\Phi(rT_c)\cdot\rho_{k,i}(r), \tag{16}$$

where $\Phi(\tau)$ is the autocorrelation function of $x(t)$ and $\rho_{k,i}(r)$ is the autocorrelation function of cross-correlation between the k-th and the i-th signals, and expressed as

$$\Phi(\tau)=\int_{-\infty}^{+\infty} x(t)\cdot x(t+\tau)\,dt \tag{17}$$

$$\rho_{k,i}(r)=\sum_{s=0}^{N-1}\theta_{k,i}(s)\cdot\theta_{k,i}(s+r). \tag{18}$$

The autocorrelation function $\Phi(rT_c)$ (r: integer) can be obtained from the power spectral density of $x(t)$ as

$$\begin{aligned}\Phi(rT_c)&=\left[\frac{1}{2\pi}\int_{-\infty}^{+\infty}X^2(\omega)\,e^{j\omega\tau}d\omega\right]_{\tau=rT_c}\\&=T_c\cdot\delta_r-\frac{1}{4}\alpha\cdot T_c\cdot(-1)^r\cdot\mathrm{Sa}(r\alpha\pi)\\&\quad-\frac{1}{8}T_c\cdot(-1)^r[\mathrm{Sa}\{(r\alpha+1)\pi\}\\&\quad+\mathrm{Sa}\{(r\alpha-1)\pi\}],\end{aligned} \tag{19}$$

where δ_r is Dirac delta function. Note that, since each signal component $h_k(t)$ is independent, each D_k is also independent and thus

$$\mathrm{Var}\left[\sum_{k=1,k\neq i}^{K}D_k\right]=\sum_{k=1,k\neq i}^{K}Var[D_k]. \tag{20}$$

Assuming that the thermal noise with single-sided spectral density N_0 is added at the input to the receiver, we obtain the variance of the thermal noise component D_n as

$$\mathrm{Var}[D_n]=\frac{N_0}{4NT_c}. \tag{21}$$

Following the above discussion, the signal-to-noise plus interference ratio (SNIR) at the output of correlator is derived as

$$\begin{aligned}SNIR_B&=D_i^2\Big/\left(\mathrm{Var}[D_n]+\sum_{k=1,k\neq i}^{K}\mathrm{Var}[D_k]\right)\\&=\left\{\frac{1}{2N^3T_c}\sum_{k=1,k\neq i}^{K}\sum_{r=-\infty}^{\infty}\Phi(rT_c)\,\rho_{k,i}(r)+\frac{N_0}{2E_b}\right\}^{-1},\end{aligned} \tag{22}$$

where $E_b=NT_cP$ is the energy of the signal for one-bit duration.

3.2 QPSK

In this subsection, SNIR for QPSK is derived through the similar procedure for BPSK. As is explained in Sect. 2, the spreading sequences with the length of $2N$ chips are assigned to the in-phase and quadrature channels, respectively. For simplicity of the analysis, information signals $b_k^I(t)$ and $b_k^Q(t)$ are assumed to be fixed at $+1$.

The k-th signal $h_k(t)$ is of the following form at the output from the receive filter:

$$\begin{aligned}h_k(t)&=\sqrt{P}\left\{\sum_{m=-\infty}^{+\infty}a_{k,m}^I\cdot x(t-mT_c-\tau_k)\right\}\\&\quad\cdot\cos(\omega_ct+\phi_k)\\&\quad+\sqrt{P}\left\{\sum_{m=-\infty}^{+\infty}a_{k,m}^Q\cdot x(t-mT_c-\tau_k)\right\}\\&\quad\cdot\sin(\omega_ct+\phi_k)\end{aligned} \tag{23}$$

where the time delay τ_k is a random variable uniformly distributed over $[0, 2NT_c]$. In this paper, the analysis will be made only for the correlated output of in-phase channel, since the same result can be obtained for the quadrature channel.

The desired signal component of the output from the correlator of the i-th signal receiver is represented as

$$D_i^I=\frac{\sqrt{P}}{2}. \tag{24}$$

The interfering component from the k-th user ($k\neq i$) D_k^I is expressed as

$$\begin{aligned}D_k^I=\frac{\sqrt{P}}{4N}\Bigg[&\cos\phi_k\sum_{q=-\infty}^{+\infty}\theta_{k,i}^{II}(q)\cdot x(qT_c-\tau_k)\\&+\sin\phi_k\sum_{q=-\infty}^{+\infty}\theta_{k,i}^{QI}(q)\cdot x(qT_c-\tau_k)\Bigg],\end{aligned} \tag{25}$$

where

$$\theta_{k,i}^{II}(q)=\sum_{l=0}^{2N-1}a_{i,l}^I\cdot a_{k,2N-q+l}^I=\theta_{k,i}^{II}(q+2N) \tag{26}$$

$$\theta_{k,i}^{QI}(q)=\sum_{l=0}^{2N-1}a_{i,l}^I\cdot a_{k,2N-q+l}^Q=\theta_{k,i}^{QI}(q+2N). \tag{27}$$

Using the above equations and the same procedure as taken for BPSK, we can obtain the variance of D_k^I:

$$\begin{aligned}\mathrm{Var}[D_k^I]=\frac{P}{64N^3T_c}\Bigg\{&\sum_{r=-\infty}^{+\infty}\Phi(rT_c)\,\rho_{k,i}^{II}(r)\\&+\sum_{r=-\infty}^{+\infty}\Phi(rT_c)\,\rho_{k,i}^{QI}(r)\Bigg\},\end{aligned} \tag{28}$$

where

$$\rho_{k,i}^{II}(r)=\sum_{s=0}^{2N-1}\theta_{k,i}^{II}(s)\,\theta_{k,i}^{II}(s+r) \tag{29}$$

$$\rho_{k,i}^{QI}(r)=\sum_{s=0}^{2N-1}\theta_{k,i}^{QI}(s)\,\theta_{k,i}^{QI}(s+r). \tag{30}$$

The variance of the thermal noise component D_n^I is

$$\mathrm{Var}[D_n^I]=\frac{N_0}{8NT_c}. \tag{31}$$

Then, the SNIR for QPSK is derived in the following:

$$SNIR_Q=\left\{\frac{1}{16N^3T_c}\sum_{k=1,k\neq i}^{K}\sum_{r=-\infty}^{+\infty}\Phi(rT_c)\,(\rho_{k,i}^{II}(r)\right.$$

$$+\rho_{k,i}^{QI}(r))+\frac{N_0}{2E_b}\Big\}^{-1}, \tag{32}$$

where E_b is the energy of the signal concerned to one-bit of the information signal $b_k^I(t)$.

4. Derivation of Approximated SNIR for Gold Sequences

In this section, Gold sequence is applied to the results of the preceding section and a simple equation representing the approximated SNIR performance is derived. For Gold sequences, the parameters $\rho_{k,i}(r)$, $\rho_{k,i}^{II}(r)$ and $\rho_{k,i}^{QI}(r)$ are predominant where $r=0$, and also the summation of them on $r\neq 0$ are very small compared to the values at $r=0$. Typical examples of $\rho_{k,i}(r)$ for Gold sequences from 9- and 10-stage shift-registers are shown in Fig. 2. On the other hand, it can be seen from (19) that the autocorrelation function $\Phi(rT_c)$ of $x(t)$ becomes maximum at $r=0$ irrespective of the value of roll-off factor α. Taking these facts into account, we can make the following approximation,

$$\sum_{r=-\infty}^{+\infty}\Phi(rT_c)\,\rho_{k,i}(r)\cong\Phi(0)\,\rho_{k,i}(0), \tag{33}$$

$$\sum_{r=-\infty}^{+\infty}\Phi(rT_c)\,(\rho_{k,i}^{II}(r)+\rho_{k,i}^{QI}(r))\cong\Phi(0)\,(\rho_{k,i}^{II}(0)+\rho_{k,i}^{QI}(0)). \tag{34}$$

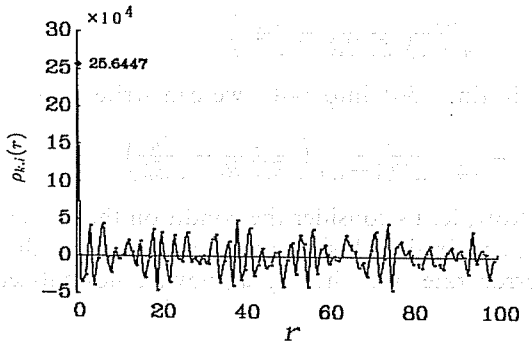

(a) 9-stage GOLD Sequence

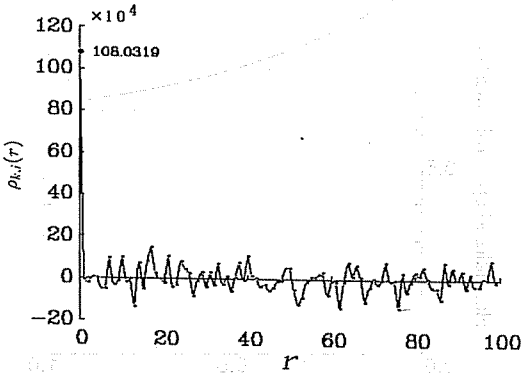

(b) 10-stage GOLD Sequence

Fig. 2 Examples of $\rho_{k,i}(r)$.

Thus (22) and (32) can be modified as follows:

$$SNIR_B\cong\Big\{\frac{1}{2N^3T_c}\Phi(0)\sum_{k=1,k\neq i}^{K}\rho_{k,i}(0)+\frac{N_0}{2E_b}\Big\}^{-1} \tag{35}$$

$$SNIR_Q\cong\Big\{\frac{1}{16N^3T_c}\Phi(0)\sum_{k=1,k\neq i}^{K}(\rho_{k,i}^{II}(0)+\rho_{k,i}^{QI}(0))+\frac{N_0}{2E_b}\Big\}^{-1}, \tag{36}$$

where from (19),

$$\Phi(0)=\Big(1-\frac{\alpha}{4}\Big)\cdot T_c. \tag{37}$$

The parameter $\rho_{k,i}(0)$ for BPSK is expressed from (18) as

$$\rho_{k,i}(0)=\sum_{s=0}^{N-1}\theta_{k,i}^2(s). \tag{38}$$

The cross-correlation values $\theta_{k,i}(s)$ for Gold sequences are given in Table 1 [4]. Using these values, we can obtain the expected value of $\rho_{k,i}(0)$ as follows:

$$E[\rho_{k,i}(0)]\cong N(N+2), \tag{39}$$

where $E[x]$ denotes the expectation of x. Similarly, the expected values of $\rho_{k,i}^{II}(0)$ and $\rho_{k,i}^{QI}(0)$ for QPSK can be obtained as

$$E[\rho_{k,i}^{II}(0)]=E[\rho_{k,i}^{QI}(0)]\cong 4N(N+1). \tag{40}$$

From (36)-(40), $SNIR_B$ and $SNIR_Q$ can be approximated as

$$SNIR_B\cong\Big\{\frac{N+2}{2N^2}\Big(1-\frac{\alpha}{4}\Big)(K-1)+\frac{N_0}{2E_b}\Big\}^{-1}, \tag{41}$$

$$SNIR_Q\cong\Big\{\frac{N+1}{2N^2}\Big(1-\frac{\alpha}{4}\Big)(K-1)+\frac{N_0}{2E_b}\Big\}^{-1}. \tag{42}$$

Since N is much larger than two in general, $SNIR_B$ and $SNIR_Q$ are nearly equal to each other, and expressed for both cases as

$$SNIR\cong\Big\{\frac{K-1}{2N}\Big(1-\frac{\alpha}{4}\Big)+\frac{N_0}{2E_b}\Big\}^{-1}. \tag{43}$$

Table 1 Cross-correlation values for Gold sequences.

Number of stage of shift register	$\theta_{k,i}(s)$	occurrence probability
M: odd number	$-(2^{\frac{M+1}{2}}+1)$	~ 0.25
	-1	~ 0.5
	$+(2^{\frac{M+1}{2}}-1)$	~ 0.25
M: even number*	$-(2^{\frac{M+2}{2}}+1)$	~ 0.125
	-1	~ 0.75
	$+(2^{\frac{M+2}{2}}-1)$	~ 0.125

* Irreducible by 4

5. Examples of Application

5. 1 Bit Error Rate Performance

The correlator output consists of the desired signal, interference, and noise components. The noise component D_n has Gaussian distribution, as the noise input to the receiver is Gaussian. When the number of the signals K is large enough, the central limit theorem ensures that the interference component, sum of independent random values D_k, can be also assumed to be Gaussian. In such a case, we can evaluate the bit error rate performance P_e of the system by SNIR obtained in the previous section as

$$P_e=\frac{1}{2}\mathrm{erfc}(\sqrt{SNIR/2}), \tag{44}$$

where, erfc(•) is the complementary error function given by

$$\mathrm{erfc}(x)=\frac{2}{\sqrt{\pi}}\int_x^{\infty} e^{-y^2}dy. \tag{45}$$

Note that the bit error rate performance is the same for BPSK and QPSK systems when the signal power, the system bandwidth and the data rate are the same.

The curves drawn in Fig. 3 are the numerical examples given by (44) with (43), where the Gold sequences with the period 1023 chips is employed. The simulation result by [5], in which the actual distribution of the cross correlation of the signals is considered, is also shown by the dots in the figure. Comparing the estimated bit error rate and the simulation result, we can confirm that the SNIR derived in the previous section is a good measure of the performance.

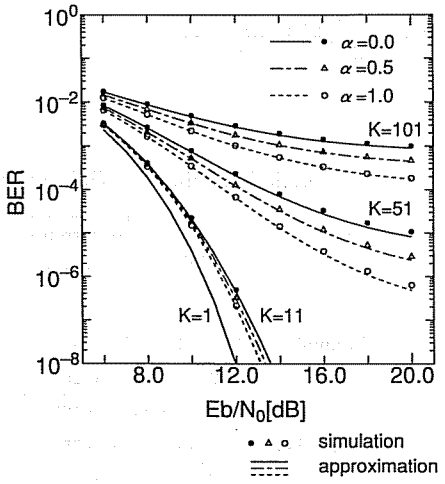

Fig. 3 Bit error rate performance.

5. 2 Spectral Efficiency

Equation (43) indicates that *SNIR* becomes maximum where the roll-off factor of the cosine roll-off filter is 1.0 for given T_c. In this subsection, we evaluate the effect of the roll-off factor from another point of view, the spectral efficiency. The spectral efficiency η is defined as follows: [6]

$$\eta=\frac{KR_b}{W_s}\ \text{[bit/sec/Hz]}, \tag{46}$$

where R_b is each user's bit rate, and W_s is the bandwidth assigned to the system.

Assuming the Nyquist spectrum shaping is adopted, we obtain R_b from (4) as

$$R_b=\frac{W_s}{N(1+\alpha)}, \tag{47}$$

and substituting into (46) we obtain

$$\eta=\frac{K}{N(1+\alpha)}. \tag{48}$$

When the number of users K is much larger than one, *SNIR* in (43) is approximated as

$$SNIR\cong\left\{\frac{K}{2N}\left(1-\frac{\alpha}{4}\right)+\frac{N_0}{2E_b}\right\}^{-1}. \tag{49}$$

From (49) we obtain the maximum number of users as

$$K=\frac{8N}{4-\alpha}\left(\frac{1}{SNIR}-\frac{N_0}{2E_b}\right). \tag{50}$$

Substituting (50) into (48), we can write η as

$$\eta=\frac{8}{(4-\alpha)(1+\alpha)}\left(\frac{1}{SNIR}-\frac{N_0}{2E_b}\right). \tag{51}$$

Now, let us consider the condition that *SNIR* and E_b/N_0 are fixed. This is equivalent to saying that the bit error rate and the signal power, normalized by

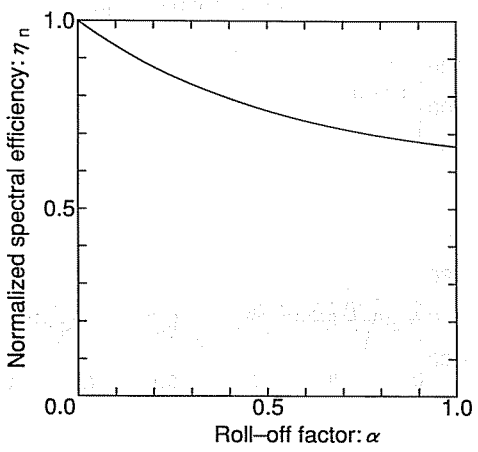

Fig. 4 Normalized spectral efficiency.

noise spectral density, are given. Under this condition, $(1/SNIR-N_0/2E_b)$ which corresponds to the amount of noise due to the interferences from other channels becomes constant and the spectral efficiency normalized by the value for the roll-off factor $\alpha=0$ is expressed as

$$\eta_n=\frac{4}{(4-\alpha)(1+\alpha)}, \tag{52}$$

which is plotted in Fig. 4. As seen in this figure, the spectral efficiency decreases as the roll-off factor increases.

6. Conclusion

In this paper, the signal-to-noise plus interference ratio (SNIR) of asynchronous band-limited DS/SSMA systems has been derived analytically for BPSK and QPSK systems. For band-limitation, Nyquist filtering is employed, because this type of filtering is most commonly used for transmission of digital signals. The SNIR is evaluated under consideration of the cross-correlation characteristics of spreading sequences. The simple approximation of SNIR is also given for the systems with Gold sequence.

The effects of band-limitation is an important issue for practical DS/SSMA systems: the numerous signals transmitted at the same time could give the serious interference to the systems in adjacent frequency bands, even though the out-of-band emission of each signal is small. The analytical expressions of SNIR derived in this paper are simple and useful for the estimation of the performance of such practical DS/SSMA systems with the band-limitation. In addition to the derivation of SNIR, the bit error rate performance and spectral efficiency are also evaluated.

The results indicate that the SNIR performances are almost the same between BPSK and QPSK. This fact suggests to us that there is no need to employ QPSK. It should be noted, however, that the number of chips for one-symbol duration of QPSK signal is twice as many as for BPSK signals under the same data rate and the system bandwidth. This implies that the larger number of spreaidng sequences may be available for assigning to users in the QPSK systems. We can also expect an improvement of performance in QPSK by the adoption of an error correcting code with the same length of spreading sequence as in BPSK.

Acknowledgement

The authors would like to thank Mr. M. Shida for his cooperation. This research has been made under the support of KDD R&D Laboratories and Fujitsu Laboratories Ltd..

References

[1] Miyakawa, H. and Imai, H., "Pulse waveform in the asynchronous CDM communications," *Record of Joint Convention of Four Institutes Associated with Elect. Eng.*, 2017, 1968.

[2] Geraniotis, E. and Ghaffari, B., "Performance of binary and quaternary direct-sequence spread-spectrum multiple-access systems with random signature sequences," *IEEE Trans. Commun.*, vol. 39, no. 5, pp. 713-724, May 1991.

[3] Gaudenzi, R. D., Elia, C. and Viola, R., "Bandlimited quasi-synchronous CDMA: A novel satellite access technique for mobile and personal communication systems," *IEEE JASC.*, vol. 10, no. 2, pp. 328-343, Feb. 1992.

[4] Gold, R., "Maximum recursive sequences with 3-valued recursive cross-correlation functions," *IEEE Trans. Inf. Theory*, vol. IT-14, no. 1, pp. 154-156, Jan. 1968.

[5] Sawada, M., Katayama, M. and Ogawa, A., "Effect of Nonlinear Amplifiers of Transmitters in the CDMA System using Offset-QPSK," *IEICE Technical Report*, SST92-85, Mar. 1993.

[6] Viterbi, A. J., "When not to spread spectrum—A sequel," *IEEE Commun. Mag.*, vol. 23, pp. 12-17, Apr. 1985.

Takafumi Shibata was born in Aichi in 1968. He received the B.E. and M.E. degrees from Nagoya University in 1990 and 1992, respectively. He is presently with NTT TOKAI Mobile Communications Network Inc.

Masaaki Katayama was born in Kyoto in 1959. He received the B.E., M.E. and Dr.Eng. degrees from Osaka University in 1981, 1983, and 1986, respectively. In 1986, he was an Assistant Professor at Toyohashi University of Technology, and had been a Lecturer at Osaka University from 1989 to 1992. Since 1992 he has been an Associate Professor at Nagoya University. His current research interests include spread-spectrum modulation schemes, satellite communications, nonlinear digital modulations, coded modulations, and computer networks. He received the IECE Shinohara Memorial Young Engineer Award in 1986. Dr. Katayama is a member of IEEE and the Information Processing Society of Japan.

Akira Ogawa was born in Nagoya in 1937. He received the B.E. and Dr.Eng. degrees from Nagoya University in 1960 and 1984, respectively. In 1961 he joined KDD Research and Development Laboratories. From 1981 to 1985 he was the Deputy Director of KDD Laboratories. From 1985 to 1988 he was the Director of Sydney Office of KDD. Since 1988 he has been a Professor at Nagoya University. He has been engaged in research mainly on digital communication technologies and spread-spectrum modulation schemes to be applied to satellite communications, mobile communications, and radiodetermination. Dr. Ogawa is a member of IEEE and IREE Australia.